Functional muscle synergies constrain force production during postural tasks

J. Lucas McKay, *Emory University*
Lena Ting, *Emory University*

Journal Title: Journal of Biomechanics
Volume: Volume 41, Number 2
Publisher: Elsevier: 12 months | 2008-01-01, Pages 299-306
Type of Work: Article | Post-print: After Peer Review
Publisher DOI: 10.1016/j.jbiomech.2007.09.012
Permanent URL: https://pid.emory.edu/ark:/25593/v1z92

Final published version: http://dx.doi.org/10.1016/j.jbiomech.2007.09.012

HHS Public Access
Author manuscript
J Biomech. Author manuscript; available in PMC 2015 March 05.

Published in final edited form as:
J Biomech. 2008 ; 41(2): 299–306. doi:10.1016/j.jbiomech.2007.09.012.

Functional muscle synergies constrain force production during postural tasks

J. Lucas McKay[a] and **Lena H. Ting**[b,*]

[a]School of Electrical and Computer Engineering, Georgia Institute of Technology, Atlanta, GA, USA

[b]The Wallace H. Coulter Department of Biomedical Engineering at Georgia Tech and Emory University, 313 Ferst Drive, Atlanta, GA, 30322-0535, USA

Abstract

We recently demonstrated that a set of five functional muscle synergies were sufficient to characterize both hindlimb muscle activity and active forces during automatic postural responses in cats standing at multiple postural configurations. This characterization depended critically upon the assumption that the endpoint force vector (synergy force vector) produced by the activation of each muscle synergy rotated with the limb axis as the hindlimb posture varied in the sagittal plane. Here, we used a detailed, 3D static model of the hindlimb to confirm that this assumption is biomechanically plausible: as we varied the model posture, simulated synergy force vectors rotated monotonically with the limb axis in the parasagittal plane ($r^2 = 0.94 \pm 0.08$). We then tested whether a neural strategy of using these five functional muscle synergies provides the same force-generating capability as controlling each of the 31 muscles individually. We compared feasible force sets (FFS) from the model with and without a muscle synergy organization. FFS volumes were significantly reduced with the muscle synergy organization ($F = 1556.01$, $p \ll 0.01$), and as posture varied, the synergy-limited FFSs changed in shape, consistent with changes in experimentally-measured active forces. In contrast, nominal FFS shapes were invariant with posture, reinforcing prior findings that postural forces cannot be predicted by hindlimb biomechanics alone. We propose that an internal model for postural force generation may coordinate functional muscle synergies that are invariant in intrinsic limb coordinates, and this reduced-dimension control scheme reduces the set of forces available for postural control.

Keywords

Musculoskeletal model; Muscle Synergies; Endpoint force; Muscle noise; Feasible force set

---

*Corresponding author: (tel) +1 404-894-5216; (fax) +1 404-385-5044, lting@emory.edu (Lena H. Ting).

Introduction

A common finding among studies of the neural control of movement is "dimensional collapse," whereby the behavior of neuromechanical systems that are in theory highly redundant (Bernstein 1967) and computationally formidable to control can be described with only a few degrees of freedom (Flash and Hochner 2005; Grasso et al. 1998; Sanger 2000; Zatsiorsky et al. 2003). However, despite this apparent motor abundance, recent studies of muscle coordination have demonstrated that the superposition of a few muscle activation patterns, defined as muscle synergies, is sufficient to describe muscular activity during many natural behaviors in humans and animals (Cheung et al. 2005; Krishnamoorthy et al. 2003; Poppele and Bosco 2003; Ting and Macpherson 2005; Tresch et al. 1999).

The hierarchical structure suggested by these results has provided substantial new insight into the neural control of movement, however, comparably few studies have examined muscle synergies quantitatively from the perspective of biomechanical function (e.g., Loeb et al. 2000; Raasch and Zajac 1999; Valero-Cuevas 2006). Comparing muscle synergies across subjects or animals, for example, is difficult not only because of experimental limitations (e.g., electrode placement) but also, because muscle synergies that appear distinct may be functionally equivalent due to biomechanical redundancy. Similarly, because the number of synergies cannot be controlled in experiments, estimating the number of synergies that are sufficient for task performance is an open question, albeit an important one from the perspective of rehabilitation (Latash and Anson 2006).

In a recent study (Torres-Oviedo et al. 2006), we demonstrated that electromyographic and kinetic data from automatic postural responses in cats could be simultaneously decomposed into a small set of five "functional" muscle synergies, which specify both a fixed pattern of hindlimb muscle activation (a muscle synergy) and a correlated "synergy force vector" at the ground. Variation in the muscle activation patterns and forces produced when the cats stood in different postural configuration (anterior-posterior "stance distances," Macpherson 1994) could be accounted for by the same muscle synergies if we assumed that the forces generated by each muscle synergy rotated with the limb axis as it varied in the sagittal plane. This result was compelling because it suggests that an internal model (Kawato 1999; Shadmehr and Mussa-Ivaldi 1994) for limb force production during postural control coordinates synergy force vectors that are invariant in the intrinsic coordinates of the limb, although the postural task itself - generating an appropriate net response force at the ground with all four limbs - is based in extrinsic coordinates.

The first aim of the present work was to verify whether the rotation of synergy force vectors implicit in our analysis of the experimental data was feasible in the context of a detailed musculoskeletal model of the cat hindlimb (Burkholder and Nichols 2004; McKay et al. 2007). While our prior analysis demonstrated that the measured EMG and force components could be correlated via the assumed muscle synergy to endpoint force transformation, we could not demonstrate that this relationship was biomechanically causal. In this study, synergy force vectors identified in the control posture of each animal from the previous work (Torres-Oviedo et al. 2006) were used as source data, and simulated muscle synergies corresponding to each hypothesized synergy force vector were determined with numerical optimization (e.g., Crowninshield and Brand 1981; Harris and Wolpert 1998; Kurtzer et al. 2006; Valero-Cuevas et al. 1998). We then applied these muscle synergies to the model in other postures to test whether the resulting force vectors were oriented consistently with respect to the limb axis.

The second aim of the present work was to assess the impact of a muscle synergy organization on the functional capabilities of the hindlimb during postural control. We tested the hypothesis that constraining the muscles in the model to be activated by a few muscle synergies would limit the model's total force-production capacity. We quantified the force-production capacity of the model using feasible force sets ("FFS," Valero-Cuevas et al. 1998). Each FFS is a convex manifold in three-dimensional "force space;" the length of the vector from the origin to any point on the FFS represents the maximum force that can generated by the model in that direction, subject to limits on individual muscle forces. The FFS is a useful descriptor because neural deficits reduce its volume and influence its shape (Kuxhaus et al. 2005). We computed FFSs across postures assuming 1) control of individuated muscles limited only by each muscles maximum force (nominal FFS), and 2) control only of the simulated muscle synergies (synergy-limited FFS). We then compared the FFSs from the two conditions (cf. Valero-Cuevas 2006) to identify systematic changes; a reduction in FFS volume associated with the synergy constraint, for example, indicates the synergy organization limits the overall force-production capacity, similar to a neuromuscular deficit. Finally, we investigated whether the stereotyped, posture-dependent changes observed in postural force production (the "force constraint strategy," Macpherson 1994) were predicted by posture-dependent changes in the nominal or synergy-limited FFS shape.

Methods

We used a static musculoskeletal model of the cat hindlimb (McKay et al. 2007) and kinematic and kinetic data of three cats performing a horizontal translation balance task at four (cats *Bi* and *Ru*) or three (cat *Ni*) postural configurations to simulate functional muscle synergies based on those of Torres-Oviedo et al. (2006). Model postures approximating the average background period kinematics of each animal in each postural configuration (11 in total) were calculated as in (McKay et al. 2007). Due to practical limitations we could not use previously reported muscle synergies directly (see Appendix A). Therefore, muscle activation patterns that could produce each of the five synergy force vectors reported from the control ("preferred") posture in each animal were determined using two optimization criteria drawn from the literature: "minimum-noise" optimization and "maximum-force" optimization.

We examined the endpoint force vectors of these simulated muscle synergies as hindlimb postural configuration varied to test the assumption (Torres-Oviedo et al. 2006) that changes in these vectors would be confined primarily to rotation in the sagittal plane. With this tested, we conducted an FFS analysis to assess whether a muscle synergy organization based on our simulated synergies would impact the force-production capability of the model by reducing FFS volume. A total of three FFSs were calculated for each of the 11 animal/posture combinations; first assuming individuated control of muscles (nominal FFS), then assuming only individuated control of the simulated synergies from the minimum-noise optimization (minimum-noise synergy-limited FFS), and last, assuming only control of the simulated synergies from the maximum-force optimization (maximum-force synergy-limited FFS). Finally, we compared the nominal and synergy-limited FFSs with experimental postural force data to determine whether the stereotyped, posture-dependent changes observed in postural forces were qualitatively predicted by posture-dependent changes in the FFSs. Statistical tests were considered significant at $p < 0.05$ (Appendix B).

Hindlimb Model

The 3-dimensional hindlimb model is presented in detail in (McKay et al. 2007). Briefly, the model is a matrix equation relating 31-element muscle excitation vectors $\vec{e}$ to the six-element force and moment system $\vec{F}$ produced at the endpoint, approximated as the metatarsal-phalangeal joint:

$$\vec{F}=\left(J(\vec{q})^T\right)^{+}R(\vec{q})\,F_O F_{AFL}(\vec{q})\,\vec{e} \quad (1)$$

Where the vector $\vec{q}$ is comprised of the model's seven rotational degrees of freedom at the hip, knee, and ankle; $(J(\vec{q})^T)^+$ is the pseudoinverse transpose of the geometric system Jacobian, $R(\vec{q})$ is the moment-arm matrix, F_O is the diagonal matrix of maximal muscle forces, and $F_{AFL}(\vec{q})$ is the diagonal matrix of scaling factors based on active muscle force-length characteristics. Muscle moment arm values and fiber lengths were determined with SIMM software (Musculographics, Inc., Santa Rosa, CA).

Muscle Synergies

In our muscle synergy analysis (Torres-Oviedo et al. 2006; Tresch et al. 1999), muscle excitation vectors $\vec{e}$ are produced by the linear combination of a few non-negative muscle synergies $\vec{w_1}, \vec{w_2}, K, \vec{w_{NSYN}}$, where the number of muscle synergies N_{SYN} is fewer than the number of muscles N_{MUS}. Each muscle synergy, $\vec{w_i}$, defines a fixed pattern of activation across multiple muscles. The contribution of each muscle synergy to any given postural response is scaled by an activation coefficient, c_i. Therefore, the nervous system is limited to producing only N_{SYN} patterns of muscle activation. However, each muscle can belong to multiple muscle synergies, and multiple muscle synergies can be active simultaneously, so the net pattern of muscle activation, $\vec{e}$, is the sum of activations due to each synergy. In matrix form, this relationship is:

$$\vec{e}=W\vec{c} \quad (2)$$

Where $\vec{w_1}, \vec{w_2}, K, \vec{w_{NSYN}}$ are the columns of W and $\vec{c}$ is a vector of synergy activation coefficients. Combining Eqs. 1 and 2 yields an expression for the force and moment system $\vec{F_c}$ due to synergy activation $\vec{c}$:

$$\vec{F}_c=\left(J(\vec{q})^T\right)^{+}R(\vec{q})\,F_O F_{AFL}(\vec{q})\,W\vec{c} \quad (3)$$

Simulated muscle synergies based on experimentally measured synergy force vectors from the control posture of each cat were determined with two different linear optimization criteria – “minimum-noise” (Crowninshield and Brand 1981; Harris and Wolpert 1998; Kurtzer et al. 2006) and “maximum-force” (Valero-Cuevas et al. 1998) optimization (Appendix A).

Nominal and Synergy-Limited Feasible Force Sets

Methods for constructing the nominal FFSs using individuated muscle control have been described in our previous work (McKay et al. 2007). Briefly, the muscle excitation $\vec{e}$ producing the largest possible force projection in each of 1000 directions distributed on the unit sphere were calculated using linear programming subject to the constraint that muscle activations varied between 0 and 1:

$$0 \leq e_j \leq 1, \quad j=1,2,\mathrm{K},N_{MUS} \quad (4)$$

The FFS was then defined as the smallest three-dimensional convex polygon that encompassed these 1000 force projections. It was determined using the *convhull* package in Matlab.

Synergy-limited FFSs were constructed using an analogous procedure. For each synergy-limited FFS, the synergy activation vector $\vec{c}$ producing the maximal biomechanically feasible force in each of 1000 directions distributed on the unit sphere was calculated using linear programming subject to the constraint (Eq. 4) and the additional non-negativity constraint

$$0 \leq c_k, \quad k=1,2,\mathrm{K},N_{SYN} \quad (5)$$

Results

Simulated synergy force vectors rotated monotonically with the limb axis in the sagittal plane as postural configuration varied, supporting the assumption implicit in the analysis of Torres-Oviedo et al. (2006) (Fig. 1). Synergy force vector angles were more highly correlated to limb axis angles in the sagittal plane ($r^2 = 0.94 \pm 0.08$, $\mu \pm \sigma$) than in the horizontal plane ($r^2 = 0.75 \pm 0.25$). The slopes of the regression lines were near unity in the sagittal plane (0.86 ± 0.44) and distributed about zero in the horizontal plane (0.28 ± 0.46); a slope of 1 would indicate that synergy force vectors were fixed in the reference frame of the limb axis.

This monotonic rotation of synergy force vectors with the limb axis was independent of the optimization model used to derive the synergies. Minimum-noise and maximum-force synergy force vectors were aligned closely and differed primarily in magnitude, despite considerable differences in the muscle activation patterns from the two optimizations (Fig. 2). Large variations in muscle activity across animals have been previously demonstrated during both quiet standing and postural responses to perturbation even though the forces produced were similar (Fung and Macpherson 1995; Torres-Oviedo et al. 2006).

Nominal FFSs (Fig. 3, gray polygons) were nearly isotropic in the sagittal plane, but anisotropic and oriented along the anterior-posterior axis in the horizontal plane (cf. McKay et al. 2007). Orientation of the nominal FFSs were not affected by changes in postural configuration; regression slopes were near zero in both sagittal (0.06 ± 0.25; $r^2 = 0.77 \pm 0.15$) and horizontal planes (0.01 ± 0.03; $r^2 = 0.60 \pm 0.50$).

Synergy-limited FFSs were qualitatively very different from the nominal FFSs (Figs. 3, 4, white) and were considerably more anisotropic in both the sagittal and horizontal planes, in particular with considerably reduced posterior force magnitude. From the standpoint of synergy-limited FFS shape, the only substantial difference between the two synergy optimization criteria was that FFSs based on maximum-force synergies encompassed some boundaries of the nominal FFSs, whereas minimum-noise FFSs did not. Synergy-limited FFSs rotated with the limb axis as posture varied, primarily in the sagittal plane (slope=1.41 ± 2.32; $r^2 = 0.92 \pm 0.05$ (sagittal); slope=0.33 ± 0.17; $r^2 = 0.75 \pm 0.14$ (horizontal)).

Changes in the synergy-limited FFS as posture varied (Fig. 4) were qualitatively similar to the changes in the distributions of active postural forces measured experimentally (Macpherson 1994). In the sagittal plane, active forces and synergy-limited FFSs both rotated closely with the limb axis. In the horizontal plane, active forces and synergy-limited FFSs were elongated along a posterior diagonal axis at “long” posture and more widely distributed, with increased anterior force magnitude at “short” and “shortest” postures; these stereotypical changes have been described previously as the “force constraint strategy” (Macpherson 1988).

Multiple ANOVA (Fig. 5) revealed that the synergy organization caused a highly significant reduction in FFS volume ($F = 1556.01$, $p \ll 0.005$). Tukey-Kramer pairwise comparisons applied post-hoc detected significant differences between the synergy-limited FFS volumes and nominal FFS volumes but no difference ($p > 0.05$) between the two optimization criteria. There was a significant main effect of stance distance ($F = 4.47$, $p < 0.012$); post-hoc tests revealed that FFS volume was highest in preferred posture. No effect of animal was detected ($F = 1.53$, $p > 0.22$). To increase statistical power, separate ANOVAs were performed to test the effect of posture on the three (nominal, minimum-noise, maximum-force) datasets; these results indicated significant effects of posture on the nominal FFS volumes ($F = 11.8$, $p < 0.004$) but not on the synergy-limited FFS volumes ($F = 0.31$, $p < 0.82$; $F = 0.25$, $p < 0.86$).

Discussion

The primary motivation of this work was to demonstrate the feasibility of the functional muscle synergy architecture proposed in our previous, experimental study (Torres-Oviedo et al. 2006) in the context of a detailed biomechanical model. Here we show that simulated synergy force vectors rotate monotonically with the limb axis in the sagittal plane as posture varies (Fig. 1), which was a critical assumption of our prior functional muscle synergy analysis. This result is important because it suggests that muscle synergies can be coordinated throughout the workspace to perform functional tasks in extrinsic coordinates with a parsimonious internal model based on a polar coordinate transformation. In the case of balance control, the orientation of the gravitational vector remains fixed while the orientations of the synergy force vectors vary with postural configuration. This type of computation is documented in the nervous system; for example, a cascade of polar transformations occurs in the first stages of voluntary reaching (Flanders and Soechting 1990). It is thought that the initial proprioceptive frame for the transformation – at the level of the dorsal spinocerebellar tract – is likely a polar scheme based on limb length and orientation (Bosco et al. 1996; Poppele et al. 2002). Mechanistically, this transformation does not have to be explicit; as a neural substrate capable of computation in different reference frames has been demonstrated (Avillac et al. 2005).

The second result of this work is that we demonstrate the muscle synergy organization comes at a "cost" in terms of the force-production capability of the limb. When the synergy architecture was imposed, it caused a dramatic reduction in FFS volume (Fig. 3–5). This indicates that large regions of the FFS are inaccessible with only the synergies recruited for postural control. Based on this result we predict that tasks like locomotion will recruit additional synergies to reach the remainder of the FFS. Synergies that are "shared" among tasks and "specific" to particular tasks have been identified in other animal and human preparations (d'Avella and Bizzi 2005; Krishnamoorthy et al. 2004). However, it is only by examining muscle synergies in a biomechanical context that we are able to compactly illustrate why this might be the case.

The considerable changes in both FFS volume and shape associated with the synergy organization also suggest it may prove valuable to consider the implications of muscle synergies when using models to predict behaviors involving submaximal forces, as opposed to "maximal" tasks (e.g., Kargo et al. 2002; Kuo and Zajac 1993; Raasch et al. 1997; Valero-Cuevas et al. 1998), where behavior is likely limited by biomechanics alone. The nominal FFS has been demonstrated as a good predictor of endpoint force in such tasks, for example for forces ranging between 200 and 650 N in the human lower limb (Schmidt et al. 2003) and maximal forces in the finger (Valero-Cuevas et al. 1998). In contrast, we have previously demonstrated that the nominal FFS is a weak predictor of postural forces in preferred posture (McKay et al. 2007). Since postural forces are small (~1–2 N and ~10 N in the horizontal and sagittal planes, respectively) compared to the biomechanical limits represented by the FFSs, the same endpoint forces vectors could have been used in all of the postural configurations if the animals used individuated muscle control. Therefore the changes in the postural forces are not necessitated by the biomechanics of the limb, but appear to arise due to a neural constraint on muscle coactivation in the form of the proposed muscle synergy organization. When we overlaid the experimental active postural response forces and the synergy-limited FFSs, we noted favorable agreement throughout the workspace (Fig. 4), suggesting that neural strategy of using the same muscle synergies across a range of postural configurations predominates the behavior.

These results were generally independent of the optimization criteria used to derive the synergies. While both optimization criteria used here predict behavior in some circumstances (Crowninshield and Brand 1981; Kurtzer et al. 2006; Valero-Cuevas 2000), the primary reason for selecting these particular criteria from the many models of their type that have been proposed (Crowninshield and Brand 1981) was the drastically different solutions they produce (Fig. 2). Although the specific criterion that best predicts postural muscle activation patterns is unknown, we can hypothesize that any function laying between the extremes of penalizing muscle activation relatively drastically ("minimum-noise") or not at all ("maximum-force") would yield similar results. Experimentally, we observe similarities in synergy force vectors across individuals, yet marked differences in the muscle synergy patterns that are used consistently by each individual (e.g, d'Avella and Bizzi 2005; Torres-Oviedo et al. 2006; Torres-Oviedo and Ting 2007). These results corroborate the idea that the different muscle activation patterns across individuals may not necessarily indicate differences in force output.

Energetic optimality has historically been an elegant guiding principle in the study of movement (cf. Alexander 1989; Hoyt and Taylor 1981). When examining the motor hierarchy, both biomechanical and neural optimality principles may be simultaneously active. We noted that the volume of the nominal FFS, which reflects biomechanical limitations on force production, was significantly higher at the preferred posture (Fig. 5), consistent with the idea that the kinematics of this self-selected posture optimize this criterion. Similarly, Fung and Macpherson (1995) used an inverse dynamic analysis to demonstrate that the preferred posture kinematics minimize total joint torques for antigravity support. At other postures, the limb is levered at the girdle, preserving the intralimb geometry and locally minimizing joint torques. Similar kinematic invariance has been demonstrated repeatedly across species (Helms-Tillery et al. 1995; Sumbre et al. 2006). Therefore, we were surprised that the volume of the synergy-limited FFS, which reflects the combined biomechanical and neural limitations on force production for the task, did not vary significantly across postural configurations. These results suggest that synergy force vectors may be specifically selected among all possible force vectors to minimize posture-dependent changes in synergy-limited FFS volume. This is but one of many possible "neural optimality" criteria that may work in concert with kinematic criteria; the contributions of both types of mechanisms should be considered to fully understand the neuromechanical coordination of the task.

Supplementary Material

Refer to Web version on PubMed Central for supplementary material.

Acknowledgments

The authors gratefully acknowledge Gelsy Torres-Oviedo for insightful discussions and providing synergy force vector data. Cat experimental data was courtesy of Jane Macpherson. Funding for this study was provided by NIH grant HD46922. The NIH had no role in the design, performance, or interpretation of the study.

References

Alexander RM. Optimization and gaits in the locomotion of vertebrates. Physiological Reviews. 1989; 69:1199–1227. [PubMed: 2678167]

Avillac M, Deneve S, Olivier E, Pouget A, Duhamel JR. Reference frames for representing visual and tactile locations in parietal cortex. Nature Neuroscience. 2005; 8:941–949.

Bernstein, N. The coordination and regulation of movements. New York: Pergamon Press; 1967.

Bosco G, Rankin AM, Poppele RE. Representation of passive hindlimb postures in cat spinocerebellar activity. Journal of Neurophysiology. 1996; 76:715–726. [PubMed: 8871193]

Burkholder TJ, Nichols TR. Three-dimensional model of the feline hindlimb. Journal of Morphology. 2004; 261:118–129. [PubMed: 15164372]

Cheung VCK, d'Avella A, Tresch MC, Bizzi E. Central and sensory contributions to the activation and organization of muscle synergies during natural motor behaviors. Journal of Neuroscience. 2005; 25:6419–6434. [PubMed: 16000633]

Crowninshield RD, Brand RA. A physiologically based criterion of muscle force prediction in locomotion. Journal of Biomechanics. 1981; 14:793–801. [PubMed: 7334039]

d'Avella A, Bizzi E. Shared and specific muscle synergies in natural motor behaviors. Proceedings of the National Academy of Sciences of the United States of America. 2005; 102:3076–3081. [PubMed: 15708969]

Flanders M, Soechting JF. Parcellation of sensorimotor transformations for arm movements. Journal of Neuroscience. 1990; 10:2420–2427. [PubMed: 2376780]

Flash T, Hochner B. Motor primitives in vertebrates and invertebrates. Current Opinion in Neurobiology. 2005; 15:660–666. [PubMed: 16275056]

Fung J, Macpherson JM. Determinants of postural orientation in quadrupedal stance. Journal of Neuroscience. 1995; 15:1121–1131. [PubMed: 7869088]

Grasso R, Bianchi L, Lacquaniti F. Motor patterns for human gait: Backward versus forward locomotion. Journal of Neurophysiology. 1998; 80:1868–1885. [PubMed: 9772246]

Harris CM, Wolpert DM. Signal-dependent noise determines motor planning. Nature. 1998; 394:780–784. [PubMed: 9723616]

Helms-Tillery SI, Ebner TJ, Soechting JF. Task dependence of primate arm postures. Experimental Brain Research. 1995; 104:1–11. [PubMed: 7621927]

Hoyt DF, Taylor CR. Gait and the energetics of locomotion in horses. Nature. 1981; 292:239–240.

Kargo WJ, Nelson F, Rome LC. Jumping in frogs: Assessing the design of the skeletal system by anatomically realistic modeling and forward dynamic simulation. Journal of Experimental Biology. 2002; 205:1683–1702. [PubMed: 12042328]

Kawato M. Internal models for motor control and trajectory planning. Current Opinion in Neurobiology. 1999; 9:718–727. [PubMed: 10607637]

Krishnamoorthy V, Goodman S, Zatsiorsky V, Latash ML. Muscle synergies during shifts of the center of pressure by standing persons: Identification of muscle modes. Biological Cybernetics. 2003; 89:152–161. [PubMed: 12905043]

Krishnamoorthy V, Latash ML, Scholz JP, Zatsiorsky VM. Muscle modes during shifts of the center of pressure by standing persons: Effect of instability and additional support. Experimental Brain Research. 2004; 157:18–31. [PubMed: 14985897]

Kuo AD, Zajac FE. A biomechanical analysis of muscle strength as a limiting factor in standing posture. Journal of Biomechanics. 1993; 26 (Suppl 1):137–150. [PubMed: 8505348]

Kurtzer I, Pruszynski JA, Herter TM, Scott SH. Primate upper limb muscles exhibit activity patterns that differ from their anatomical action during a postural task. Journal of Neurophysiology. 2006; 95:493–504. [PubMed: 16251262]

Kuxhaus L, Roach SS, Valero-Cuevas FJ. Quantifying deficits in the 3d force capabilities of a digit caused by selective paralysis: Application to the thumb with simulated low ulnar nerve palsy. Journal of Biomechanics. 2005; 38:725–736. [PubMed: 15713293]

Latash ML, Anson JG. Synergies in health and disease: Relations to adaptive changes in motor coordination. Physical Therapy. 2006; 86:1151–1160. [PubMed: 16879049]

Lloyd DG, Besier TF. An emg-driven musculoskeletal model to estimate muscle forces and knee joint moments in vivo. Journal of Biomechanics. 2003; 36:765–776. [PubMed: 12742444]

Loeb EP, Giszter SF, Saltiel P, Bizzi E, Mussa-Ivaldi FA. Output units of motor behavior: An experimental and modeling study. Journal of Cognitive Neuroscience. 2000; 12:78–97. [PubMed: 10769307]

Macpherson JM. Changes in a postural strategy with inter-paw distance. Journal of Neurophysiology. 1994; 71:931–940. [PubMed: 8201433]

Macpherson JM. Strategies that simplify the control of quadrupedal stance. I. Forces at the ground. Journal of Neurophysiology. 1988; 60:204–217. [PubMed: 3404217]

McKay JL, Burkholder TJ, Ting LH. Biomechanical capabilities influence postural control strategies in the cat hindlimb. Journal of Biomechanics. 2007; 40:2254–2260. [PubMed: 17156787]

Poppele R, Bosco G. Sophisticated spinal contributions to motor control. Trends in Neurosciences. 2003; 26:269–276. [PubMed: 12744844]

Poppele RE, Bosco G, Rankin AM. Independent representations of limb axis length and orientation in spinocerebellar response components. Journal of Neurophysiology. 2002; 87:409–422. [PubMed: 11784759]

Raasch CC, Zajac FE. Locomotor strategy for pedaling: Muscle groups and biomechanical functions. Journal of Neurophysiology. 1999; 82:515–525. [PubMed: 10444651]

Raasch CC, Zajac FE, Ma B, Levine WS. Muscle coordination of maximum-speed pedaling. Journal of Biomechanics. 1997; 30:595–602. [PubMed: 9165393]

Sanger TD. Human arm movements described by a low-dimensional superposition of principal components. Journal of Neuroscience. 2000; 20:1066–1072. [PubMed: 10648712]

Schmidt MW, Lopez-Ortiz C, Barrett PS, Rogers LM, Gruben KG. Foot force direction in an isometric pushing task: Prediction by kinematic and musculoskeletal models. Experimental Brain Research. 2003; 150:245–254. [PubMed: 12682808]

Shadmehr R, Mussa-Ivaldi FA. Adaptive representation of dynamics during learning of a motor task. Journal of Neuroscience. 1994; 14:3208–3224. [PubMed: 8182467]

Sumbre G, Fiorito G, Flash T, Hochner B. Octopuses use a human-like strategy to control precise point-to-point arm movements. Current Biology. 2006; 16:767–772. [PubMed: 16631583]

Ting LH, Macpherson JM. A limited set of muscle synergies for force control during a postural task. Journal of Neurophysiology. 2005; 93:609–613. [PubMed: 15342720]

Torres-Oviedo G, Macpherson JM, Ting LH. Muscle synergy organization is robust across a variety of postural perturbations. Journal of Neurophysiology. 2006; 96:1530–1546. [PubMed: 16775203]

Torres-Oviedo G, Ting LH. Muscle synergies characterizing human postural responses. Journal of Neurophysiology. 2007

Tresch MC, Saltiel P, Bizzi E. The construction of movement by the spinal cord. Nature Neuroscience. 1999; 2:162–167.

Valero-Cuevas, FJ. A mathematical approach to the mechanical capabilities of limbs and fingers. Progress in Motor Control V; State College, Pennsylvania. 2006.

Valero-Cuevas FJ. Predictive modulation of muscle coordination pattern magnitude scales fingertip force magnitude over the voluntary range. Journal of Neurophysiology. 2000; 83:1469–1479. [PubMed: 10712473]

Valero-Cuevas FJ, Zajac FE, Burgar CG. Large index-fingertip forces are produced by subject-independent patterns of muscle excitation. Journal of Biomechanics. 1998; 31:693–703. [PubMed: 9796669]

van Bolhuis BM, Gielen CC. A comparison of models explaining muscle activation patterns for isometric contractions. Biological Cybernetics. 1999; 81:249–261. [PubMed: 10473849]

Zatsiorsky VM, Gao F, Latash ML. Prehension synergies: Effects of object geometry and prescribed torques. Experimental Brain Research. 2003; 148:77–87. [PubMed: 12478398]

Appendix A: Optimization Models

Practical limitations necessitated that we could not use previously reported muscle synergies directly. In particular, as no absolute normalization data (e.g., maximum voluntary contraction Lloyd and Besier 2003) was available, EMG records in (Torres-Oviedo et al.

2006) were presented in arbitrary units which were unsuitable for use in the model. In addition, the model includes a superset of the muscles studied earlier, with the addition of adductor femoris, adductor longus, flexor hallicis longus, gluteus maximus, gluteus minimus, peroneus brevis, peroneus longus, peroneus tertius, pectineus, pyrformis, quadratus femoris, tibialis posterior, vastus intermedius, and the omission of tensor fasciae latae.

To resolve these issues, simulated muscle synergies based on experimentally measured synergy force vectors from the preferred posture of each animal were determined with two different optimization models.

Given a synergy force vector $\vec{f_{wi}}$, the unique muscle synergy $\vec{w_i}$ that achieves $\vec{f_{wi}}$ while minimizing signal-dependent noise (equivalent to muscular stress, e.g., Crowninshield and Brand 1981; Harris and Wolpert 1998; Kurtzer et al. 2006) can be determined with quadratic programming. Notice that this formulation differs slightly from the "force-sharing problem" (e.g., van Bolhuis and Gielen 1999) because we consider endpoint forces as opposed to joint torques. First we partition Eq. 1 to separately consider the rows corresponding to endpoint force (A_F) and moment (A_M):

$$\begin{bmatrix} A_F \\ A_M \end{bmatrix} \equiv \left(J(\vec{q})^T\right)^+ R(\vec{q})\, F_O F_{AFL}(\vec{q}) \quad \text{(A.1)}$$

Then, $\vec{w_i}$ is given by

$$\text{minimum noise:} \begin{cases} \text{minimize:} & \vec{w}_i^{\,T} \underline{\vec{w}}_i \\ \text{such that:} & \vec{f}_{wi} = A_F \vec{w}_i \end{cases} \quad \text{(A.2)}$$

Equivalently, the unique muscle synergy $\vec{w_i}$ that maximizes feasible force in the direction of $\vec{f_{wi}}$ subject to limits on individual muscle forces (Valero-Cuevas et al. 1998) is given by

$$\text{maximum force:} \begin{cases} \text{maximize:} & \vec{f}_i \cdot (A_F \vec{w}_i) \\ \text{such that:} & \left| \vec{f}_{wi} \times (A_F \vec{w}_i) \right| = 0 \\ & 0 \le w_{ij} \le 1, \quad j = 1, 2, \mathrm{K}, N_{MUS} \end{cases} \quad \text{(A.3)}$$

Where w_{ij} denotes the jth element of $\vec{w_i}$. For convenience, the cross-product constraint of Eq. A.3 was realized as the equivalent linear equality constraint $\vec{f_{wi}} \times (\vec{A_F w_i}) = [0\ 0\ 0]^T$. Solutions $\vec{w_i}$ were subsequently normalized by their maximum value.

Notice that because muscle synergies $\vec{w_i}$ are normalized to unit maximum value, enforcing the constraint (Eq. 4) implicitly limits the elements c_k to the interval [0,1] in the synergy-limited force set calculation; this is in contrast to our experimental studies (Ting and Macpherson 2005; Torres-Oviedo et al. 2006), where c_k are allowed to assume any non-negative value.

Appendix B: Statistical Tests

A series of linear regressions was performed to identify systematic variation in the orientation of synergy force vectors, nominal FFSs, and synergy-limited FFSs as the limb moved through the workspace. Sagittal and horizontal plane orientation data were treated separately. While angles of synergy force vectors in the sagittal and horizontal planes were calculated directly, orientation of the FFSs and synergy-limited FFSs was quantified by calculating the sagittal and horizontal plane angles of the 3D vector in $[f_x\ f_y\ f_z\ ]^T$ from the origin to the FFS centroid (cf. Kuxhaus et al. 2005). Similarly, orientation of the limb itself was quantified with the sagittal and horizontal plane angles of the “limb axis,” the 3D vector in $[x\ y\ z]^T$ from the hip center to the MTP.

Multiple ANOVA was applied to the pooled FFS and synergy-limited FFS volume data. Synergy organization, stance distance, and experimental animal were tested as independent variables.

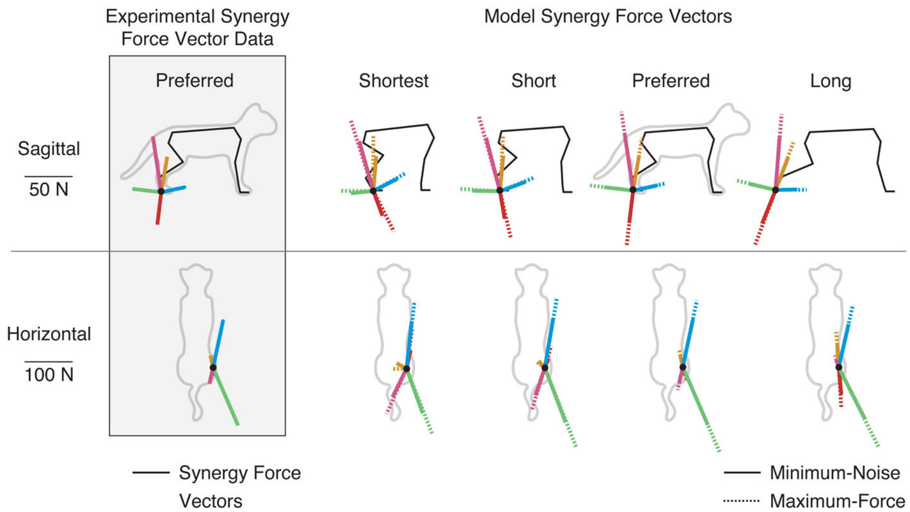

Figure 1.

Synergy force vector rotation with postural configuration. Left: synergy force vectors from the control condition (preferred posture), as presented by Torres-Oviedo et al. (2006), used as source data. Average hindlimb kinematics are shown in black. Data shown are from cat *Ru*. Right: when simulated muscle synergies based on synergy force vectors at left are applied to the model in other postural configurations (shortest, short, long), the resulting synergy force vectors rotate monotonically with the sagittal-plane limb axis. Similar results are obtained whether minimum-noise (solid) and maximum-force (dashed) optimization is used to derive the simulated muscle synergies.

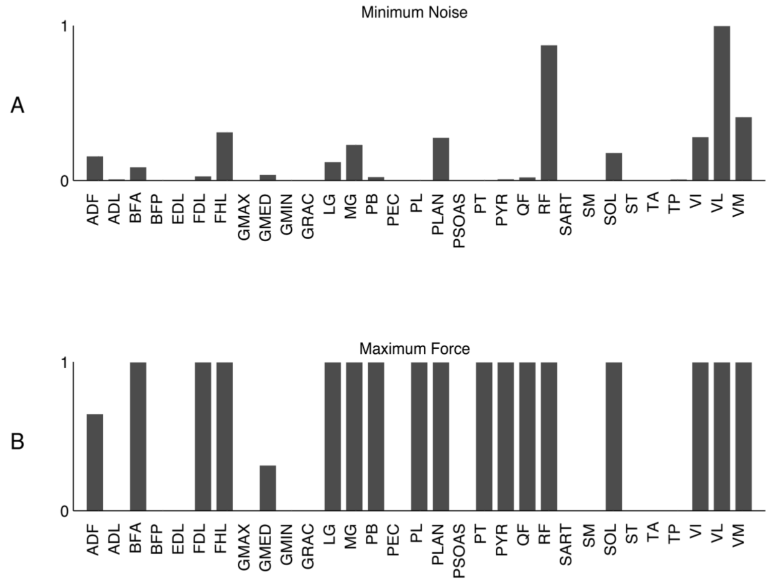

Figure 2.

Drastically different muscle synergies producing identically-oriented synergy force vectors. The simulated muscle synergies shown were calculated to produce forces aligned with the synergy force vector shown in red for cat *Ru* in preferred posture (Fig. 1) using (A) minimum-noise and (B) maximum-force optimization criteria. The minimum-noise optimization, equivalent to muscle stress minimization (Crowninshield and Brand 1981), results in less coactivation than the maximum-force optimization.

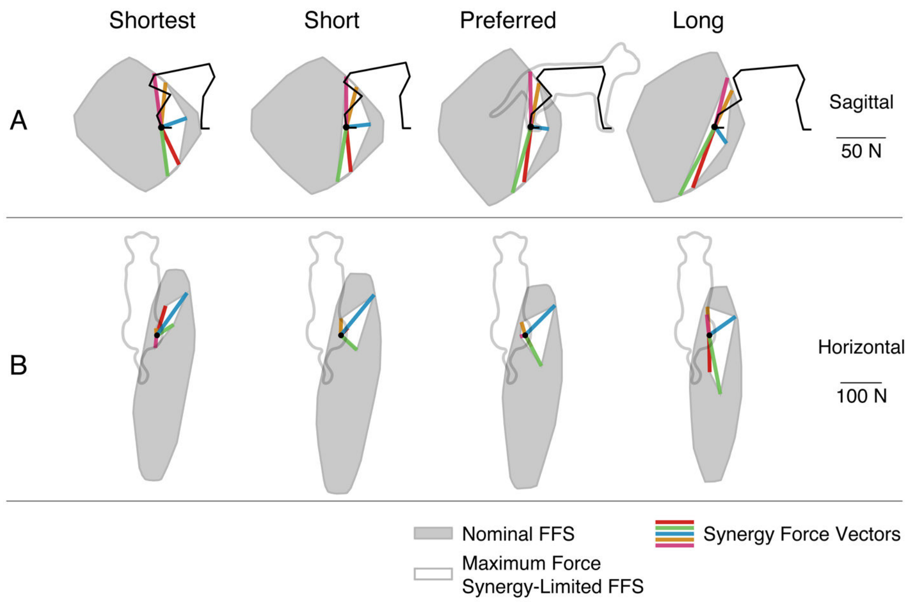

Figure 3.

Nominal FFS (gray), maximum-force synergy-limited FFS (white), and simulated maximum-force synergy force vectors (colored lines) for cat *Bi* in all postures. A: sagittal projection. B: horizontal projection. Enforcing the muscle synergy organization dramatically reduces the volume of the FFS in all postures. The synergy force vectors span the synergy-limited FFS, so that any point on the synergy-limited FFS can be reached with a linear combination of the synergy force vectors. While the nominal FFS is largely invariant across postures, the synergy-limited FFS rotates with the hindlimb axis in the sagittal plane, and changes shape acutely in the horizontal plane.

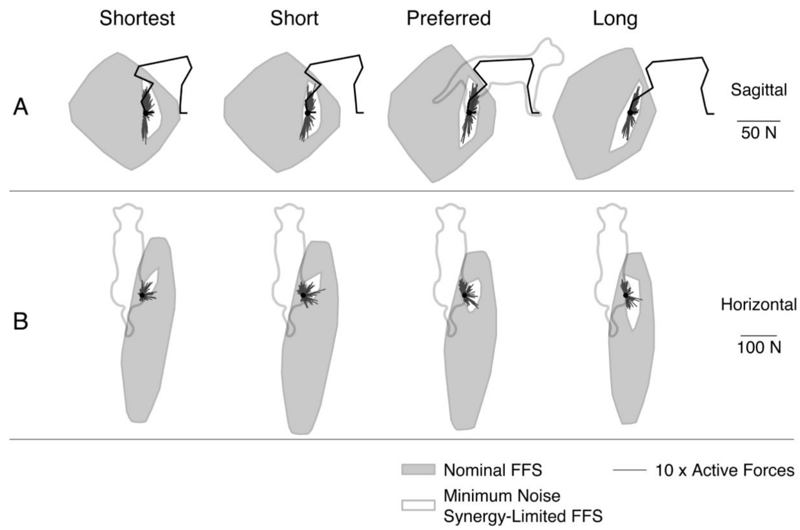

Figure 4.

Nominal FFS (gray), minimum-noise synergy-limited FFS (white), and active postural forces (dark gray; magnified 10 ×) for cat *Bi* in all postures. Active postural response forces are averaged across time windows as in Torres-Oviedo et al. (2006). A: sagittal projection. B: horizontal projection. The synergy-limited FFS is a substantially better predictor of the distribution of postural forces than the nominal FFS at all postures, Particularly in the sagittal plane, where the synergy-limited FFS rotates closely with the envelope of postural forces. While the nominal FFS predicts almost no change in force production in the horizontal plane as posture varies, the synergy-limited FFS predicts stereotypical changes along a posterior diagonal axis (downwards and to the right, in the figure) at long posture and increased anterior forces (upwards, in the figure) at shortest posture, as is observed experimentally (Macpherson 1994).

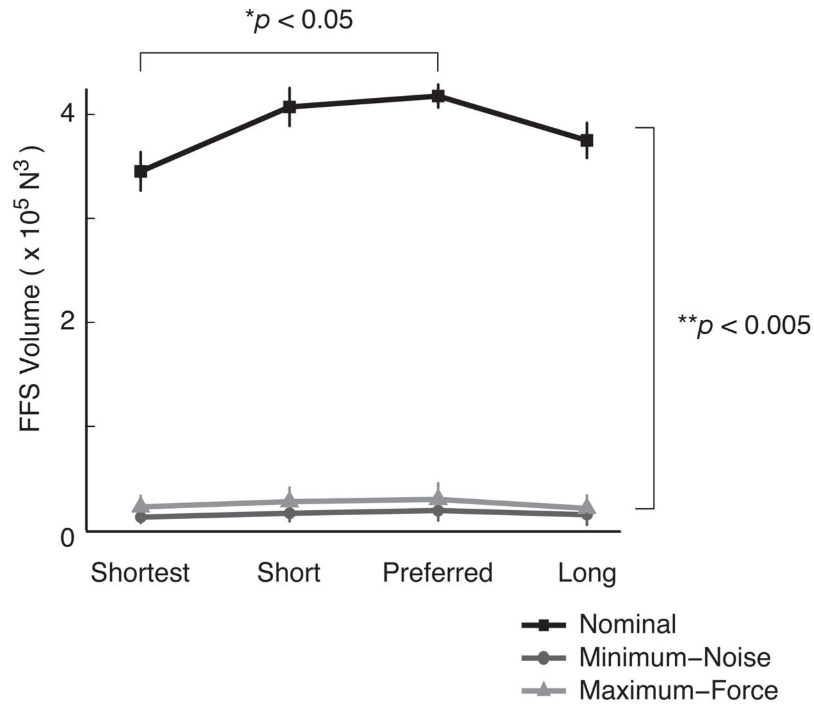

Figure 5.

Changes in nominal and synergy-limited FFS volume with posture. Data are presented as μ ± σ. Synergy-limited FFSs have significantly reduced volume (multiple ANOVA; F = 1556.01, $^{**}p \ll 0.005$) compared to nominal FFSs. Tukey-Kramer pairwise comparisons applied post-hoc detected significant differences between the synergy-limited FFS volumes and nominal FFS volumes but no difference between the two optimization criteria. There was a significant main effect of postural configuration (F = 4.47, $^{*}p < 0.012$); post-hoc tests revealed that FFS volumes in preferred posture were significantly higher than in shortest posture. No effect of animal was detected (F = 1.53, $p < 0.23$). To increase statistical power, separate ANOVAs were performed to test the effect of posture on the three (nominal, minimum-noise, maximum-force) datasets; these results indicated significant effects of postural configuration on the nominal FFS data (F = 11.8, $p < 0.004$) but not on the synergy-limited FFS data (F = 0.31, $p < 0.82$; F = 0.25, $p < 0.86$).